

Constraining the magnitude of climate extremes from time-varying instellation on a circumbinary terrestrial planet

Jacob Haqq-Misra¹, Eric T. Wolf², William F. Welsh³, Ravi Kumar Kopparapu⁴, Veselin Kostov⁴, and Stephen R. Kane⁵

¹Blue Marble Space Institute of Science, Seattle, Washington, USA.

²University of Colorado Boulder, Boulder, Colorado, USA, USA.

³San Diego State University, San Diego, California, USA.

⁴NASA Goddard Space Flight Center, Greenbelt, Maryland, USA.

⁵University of California Riverside, Riverside, California, USA.

Abstract

Planets that revolve around a binary pair of stars are known as circumbinary planets. The orbital motion of the stars around their center of mass causes a periodic variation in the total instellation incident upon a circumbinary planet. This study uses both an analytic and numerical energy balance model to calculate the extent to which this effect can drive changes in surface temperature on circumbinary terrestrial planets. We show that the amplitude of the temperature variation is largely constrained by the effective heat capacity, which corresponds to the ocean-to-land ratio on the planet. Planets with large ocean fractions should experience only modest warming and cooling of only a few degrees, which suggests that habitability cannot be precluded for such circumbinary planets. Planets with large land fractions that experience extreme periodic forcing could be prone to changes in temperature of tens of degrees or more, which could drive more extreme climate changes that inhibit continuously habitable conditions.

1 Introduction

The recent discovery of giant planets in the habitable zone of close binary stars (*e.g.*, *Welsh and Orosz* [2018] and references therein) has raised the possibility that such systems could host terrestrial planets within the liquid water habitable zone. The circumstellar liquid water “habitable zone” has received broad attention for single-star systems (*e.g.*, *Kasting et al.* [1993]; *Abe et al.* [2011]; *Kopparapu et al.* [2013]; *Kopparapu et al.* [2014], but terrestrial planets in binary systems may also be able to retain stable atmospheres with habitable surface conditions. Previous studies have calculated the boundaries of the habitable zone in circumbinary systems (also known as P-type systems [*Dvorak*, 1984]) by combining the spectral energy distributions of the host stars to determine the orbital range that can maintain stable climates for an Earth-like planet [*Kane and Hinkel*, 2012; *Haghighipour and Kaltenegger*, 2013; *Forgan*, 2013; *Cuntz*, 2013, 2015; *Wang and Cuntz*, 2019a,b; *Georgarakos and Eggl*, 2019]. Such studies demonstrate that circumbinary systems could host dynamically stable planets that maintain habitable conditions, so long as the planet has a sufficiently dense atmosphere and a method for recycling carbon between the atmosphere and interior (*i.e.*, plate tectonics). Circumbinary planets have also been argued to have enhanced habitability prospects due to reduced stellar activity and XUV radiation [*Mason et al.*, 2013].

A circumbinary planet experiences changes in instellation as the binary pair orbit one another. The orbital separation of the binary pair causes a periodic variation in incident radiation, which changes both the intensity and distribution of the incident spectral energy distribution [*Forgan et al.*, 2015]. In some cases more extreme variations in incident energy can occur when one star eclipses another (as seen by the planet); however, while these eclipses are global in extent, they only have a duration of hours. The longer period variation in radiation from the binary pair is a time-dependent factor that could alter a planet’s ability to sustain habitable conditions, even if it is otherwise situated

within the habitable zone. We refer to this periodic change in energy incident upon the planet as the circumbinary “gyration effect.”

Case studies of existing circumbinary systems suggest that this gyration effect may only exert a modest effect on global climate. (Such results corroborate other studies that have generally found modest deviations from the mean flux approximation when considering variations in a planet’s orbital eccentricity [Dressing et al., 2010; Bolmont et al., 2016; Way and Georgakarakos, 2017].) May and Rauscher [2016] examine this periodic variation in instellation for Neptune-like circumbinary planets in the Kepler-47 system by using both an energy balance model and an idealized general circulation model (GCM) to calculate the maximum temperature changes expected. May and Rauscher [2016] find that Neptune-like circumbinary planets would experience no more than one percent variation in temperature from the gyration effect. Popp and Egel [2017] use a GCM to calculate climate variations for hypothetical Earth-like planets in the Kepler-35 system and find that the global mean surface temperature changes by a few degrees at most. These results suggest that the gyration effect is unlikely to preclude habitability for planets within the circumbinary habitable zone. However, these previous efforts investigated planets with a uniform surface with a large heat capacity, which is appropriate for an ocean-covered planet or Neptune analog but may underestimate temperature variations on an Earth-like planet.

In this study, we attempt to determine the extent to which the gyration effect is capable of driving significant changes in temperature for dynamically-stable circumbinary planets that orbit within the habitable zone. We address cases where the planets transit main-sequence stars, *i.e.*, cases similar to the Kepler circumbinary planets. We use an analytic energy balance model to show that the effective heat capacity of a planet exerts the greatest control on the magnitude of the temperature variation that results from the circumbinary gyration effect. We then use a numerical energy balance model to show that the amplitude of time-dependent changes in temperature is greatest for planets with a large land fraction (and thus a lower effective heat capacity). Our results suggest that circumbinary planets with a lower ocean-to-land surface fraction that undergo strong periodic forcing are more likely to experience extreme climate change.

2 Maximum variation from periodic forcing

As the distances between a circumbinary planet and its host stars continuously vary, the planet experiences a change in instellation throughout its orbit. The amplitude of the change depends on the orbits of the binary stars and the planets (specifically the luminosity of each star, semi-major axes, and eccentricities; throughout this paper we assume co-planar orbits). The timescale of the change depends on the orbital periods of the binary, the planet, and long-term precession of the planet’s orbit. Of the known Kepler circumbinary planets, the shortest period binary is that of Kepler-47 with a period of 7.4 days, with planets b, c, and d on 49.5, 303, and 187 day orbits [Orosz et al., 2019]. The longest period host binary is that of Kepler-16, with an orbital period of 41 days [Doyle et al., 2011] and a planet on a ~ 229 day orbit. Note that the longer the period of the binary, the lower the probability of transit, and so the more difficult it is to detect a circumbinary planet. Current observations thus do not provide much constraint on the maximum orbital period of the binary. However, the stability criteria of Holman and Wiegert [1999] requires that the binary must have a period shorter than approximately one third of the planet’s orbital period in order for the planet to be dynamical stable (assuming a circular planetary orbit). In this study, we apply this stability criterion between the binary orbital period, P_{bin} , and the orbital period of the circumbinary planet, P_{cbp} , in order to constrain the extent of temperature variation on Earth-like circumbinary planets.

The maximum variation in instellation spans a wide range across the observed Kepler circumbinary systems. The most variable is Kepler-34b, which is not in the habitable zone (too hot). Kepler-34b is the most eccentric of known transiting circumbinary planets (Welsh et al. [2012]), and its eccentric orbit ($e_{cbp} = 0.182$) is a significant factor driving changes in instellation. Kepler-35b, also not in the habitable zone, has a much lower eccentricity than Kepler-34b ($e_{cbp} = 0.042$), which leads to a semiamplitude of about 15%. The circumbinary systems that are in the habitable zone (Kepler-16, 47, 453, 1647) have similar instellation semiamplitudes, less than 20% on a timescale

of a few planetary orbits. However, on a longer timescale (\sim decades to centuries) planet orbit precession can play a significant role: Kepler-16b has the most circular orbit ($e_{cbp} = 0.0069$) of the known circumbinary planets, but experiences a range in semiamplitude variation from about 17% to 28% due to evolution of its orbit. This suggests that a semiamplitude of 30% is certainly reasonable for a nearly circular orbit, and higher values as the eccentricity increases. The most eccentric Kepler circumbinary planet is the non-transiting planet KIC 7821010 b with $e \sim 0.35$ [Priv. Comm.]. Similar to that of Kepler-34 b, its change in instellation is $\sim 90\%$. But unlike Kepler-34 b, KIC 7821010 b orbits within the habitable zone (most of the time) with an average instellation equal to $\sim 68\%$ of the solar flux.

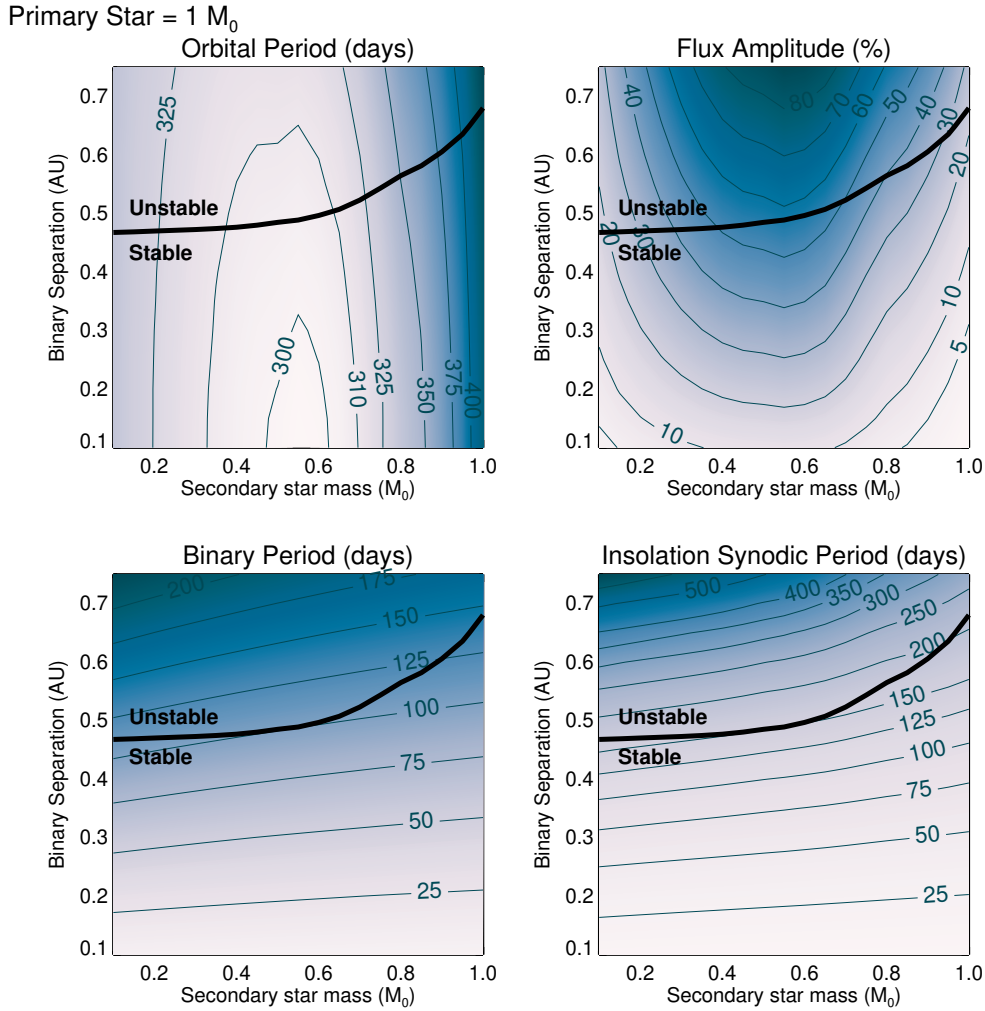


Figure 1. The orbital period of the planet (top left), flux amplitude (top right), binary orbital period (bottom left), and insolation synodic period at the planet's orbit (bottom right) depend on the binary separation and the mass of the secondary star. Calculations assume a $1 M_{\odot}$ primary and a planet in a circular circumbinary orbit with a time mean instellation of 1360 W m^{-2} . The dark curve indicates the maximum binary separation that permits a stable orbiting planet. The maximum flux amplitude of 55% occurs for a $0.5 M_{\odot}$ secondary star, which corresponds to a planetary orbital period of about 305 days, a binary orbital period of about 100 days, and an insolation synodic period of about 150 days on the planet.

We first estimate the maximum amplitude of the gyration effect for a hypothetical circumbinary system with a planet that receives the same time-mean value of stellar insolation as Earth today. We keep the mass of the primary star fixed at $1 M_{\odot}$ and vary the mass of the secondary from 0.1 to $1 M_{\odot}$, with a binary separation ranging from 0.1 to 0.75 AU. We simplify our calculations by assuming a non-eccentric orbit and solve Kepler’s laws using stellar mass-luminosity functions [Pecaut and Mamajek, 2013; Pecaut et al., 2012]. The top left panel of Fig. 1 shows the orbital period of a planet in such a circumbinary system (following Kepler’s laws), where the incident stellar flux on the planet has been fixed at the present-day Earth value of 1360 W m^{-2} . The black curve indicates the maximum binary separation that permits a planet to remain in a stable orbit at this incident flux, following the $P_{bin} \approx P_{cbp}/3$ stability criteria [Holman and Wiegert, 1999]. The amplitude of flux variation from the circumbinary pair is shown in the top left panel of Fig. 1, which indicates a maximum flux amplitude of about 55% with a secondary mass of about $0.5 M_{\odot}$ and a binary separation of about 0.5 AU.

We next determine the period of variation in instellation that corresponds to this hypothetical circumbinary system with a $1 M_{\odot}$ primary and $0.5 M_{\odot}$ secondary. The maximum flux amplitude occurs with a binary orbital period of about 100 days, as shown in the bottom left panel of Fig. 1. The planet in such a system has an orbital period of about 305 days, so the period of variation in flux is determined by the combined motion of the binary pair and circumbinary planet. The resulting insolation synodic period is shown in the bottom right panel of Fig. 1, which indicates a period of about 150 days. In our model calculations that follow, we will consider the response of a terrestrial planet in such a circumbinary system, with the period of the circumbinary gyration effect at 150 days and the maximum amplitude of flux variation at 50%. We specifically choose this extreme instellation variation scenario to examine the maximum response of the circumbinary planet’s climate, and to answer the question, “Are climate variations due to the gyration effect negligible or significant?” But note that for developing our intuition, via the analytic energy balance calculations in the next section, we use circular orbits. Much more extreme instellation variations are possible for highly eccentric orbits.

3 Analytic energy balance model

This section examines the amplitude of temperature variation due to the time-dependent circumbinary gyration effect. The analytic energy balance calculations shown below demonstrate that the effect typically causes temperature to oscillate by only a few degrees for most cases, which is consistent with previous results [May and Rauscher, 2016; Popp and Eggl, 2017]. At the same time, planets with a much lower effective heat capacity may experience tens of degrees of temperature change.

The rate of change of surface temperature, dT/dt , on a terrestrial planet depends upon the incoming stellar energy, S , the planetary Bond albedo, α , and the outgoing infrared radiative flux, F_{IR} . We can express this relationship as

$$C \frac{dT}{dt} = S(1 - \alpha) - F_{IR}, \quad (1)$$

where C is effective heat capacity of the surface and atmosphere. A simple representation of F_{IR} is the linear parameterization $F_{IR} = A + BT$, where A and B are infrared flux constants (with T in Celsius). For this problem, we are interested in a periodic variation of the incoming stellar energy. This serves as an analogy to the changes in flux for a circumbinary planet when its host stars orbit one another. We choose a simple periodic function:

$$S = S_0 (1 + \kappa \sin \omega t), \quad (2)$$

where S_0 is a constant value of incident stellar flux, ω is the angular frequency of flux variation (with $\omega = 2\pi/P_{bin}$), and κ is the amplitude of flux variation. This function is constructed to begin with a flux of $S = S_0$ at $t = 0$ and recover a single-star solution when $\kappa = 0$. We acknowledge that this sinusoidal representation of stellar flux implies a circular planetary orbit ($e_{cbp} = 0$), which would be dynamically unstable in an actual circumbinary system; however, it is possible for planet orbits

to remain stable with small non-zero eccentricities. (One way to extend this analytic model would be to develop the forcing as a real-valued Fourier series [Popp and Eggl, 2017], with a solution that corresponds to the sum of several modes. The single-mode solution developed in this paper indicates the qualitative behavior expanded from more realistic, multi-modal circumbinary orbits.) We will proceed by emphasizing that these calculations are intended to place theoretical limits on the impact of time-varying instellation on climate by using an idealized representation of the circumbinary flux variation. We can then write Eq. (1) as

$$C \frac{dT}{dt} = S_0 (1 - \alpha) [1 + \kappa \sin(\omega t)] - (A + BT). \quad (3)$$

We can solve this ordinary differential equation in order to obtain an expression for $T(t)$ that depends upon C , ω , and κ . We assume that α is constant, analogous to an ice-free and ocean-covered planet (i.e., no ice-albedo feedback).

The analytic solution to Eq. (3) is given in the Appendix, which yields an expression for the steady-state solution:

$$T(t) \approx \frac{S_0 (1 - \alpha) \kappa}{\omega C} \cos(\omega t) + T_0. \quad (4)$$

The amplitude of Eq. (4) represents the magnitude of temperature perturbations from circumbinary forcing. It is noteworthy that the infrared flux constants A and B are absent from Eq. (4), with the effective heat capacity as the primary planetary property that affects the amplitude of the gyration effect. Although the mean temperature T_0 is determined by properties of the atmosphere's composition (through the greenhouse effect, as described by A and B), the amplitude of circumbinary change in this analytic model is insensitive to changes in the greenhouse effect.

In order to apply Eq. (4) to the scenario of a circumbinary planet in the habitable zone, we assume Earth-like conditions of $T_0 = 15^\circ\text{C}$ and $C = 2.1 \times 10^8 \text{ J m}^{-2} \text{ }^\circ\text{C}^{-1}$. We are also interested in small perturbations in temperature that result from variations in instellation as the binary pair rotates, so we ignore any changes in albedo due to ice growth and assume a constant value of α . We obtain a value for albedo by setting Eq. (3) to a steady state ($dT/dt = 0$) with a fixed single star ($\omega = 0$) and solving for α when $T = T_0$, which gives $\alpha = 1 - (A + BT_0)/S_0 \approx 0.31$. (This expression for albedo assumes Earth-like values for the thermal emitted flux parameters, $A = 203 \text{ W m}^{-2}$ and $B = 2 \text{ W m}^{-2} \text{ }^\circ\text{C}^{-1}$, which are based on northern hemisphere observations [North et al., 1981].) We use this value of α to evaluate Eq. (4). Given the assumptions that went into this calculation, it should not be surprising that this is in fact similar to the measured value of $\alpha \approx 0.29$ for Earth (e.g. Stephens et al. [2015]).

Examples of solutions given by Eq. (4) are shown in Fig. 2, which includes the time variation in stellar flux (top panel) and steady-state temperature (bottom panel) for several cycles. These cases assume $P_{bin} = 150$ days ($\omega \approx 0.04 \text{ rad day}^{-1}$), with a single star control case ($\kappa = 0$) and two circumbinary cases with small amplitude ($\kappa = 0.2$) and extreme amplitude ($\kappa = 0.5$). The variation in mean planet temperature shows a lag relative to the variations in stellar flux. The lag timescale, t_{lag} , is the difference in the time between the maxima of the stellar forcing function from Eq. (2) and temperature from Eq. (13), which we can express as

$$t_{lag} = \frac{1}{\omega} \left(\frac{\pi}{2} + \arctan \frac{B}{\omega C} \right) \approx \frac{\pi}{2\omega} = \frac{P_{bin}}{4}, \quad (5)$$

where we have made the simplifying assumption $\omega C \gg B$. The lag time for climate thus depends only upon the circumbinary orbital period, rather than properties of the planet's radiative transfer variable described by B . At larger circumbinary orbital periods, the lag timescale increases and enables a delayed response of climate to periodic changes in instellation. The $P_{bin} = 150$ day circumbinary period considered in Fig. 2 corresponds to a lag timescale of $t_{lag} = 38$ days, which is long enough to induce a periodic temperature change of one to several degrees.

These calculations indicate that the gyration effect of periodic variation about the mean in incident stellar flux is capable of driving periodic change in planetary temperature. The angular frequency of flux variation, ω , (or equivalently, the period P_{bin}) determines the lag between flux

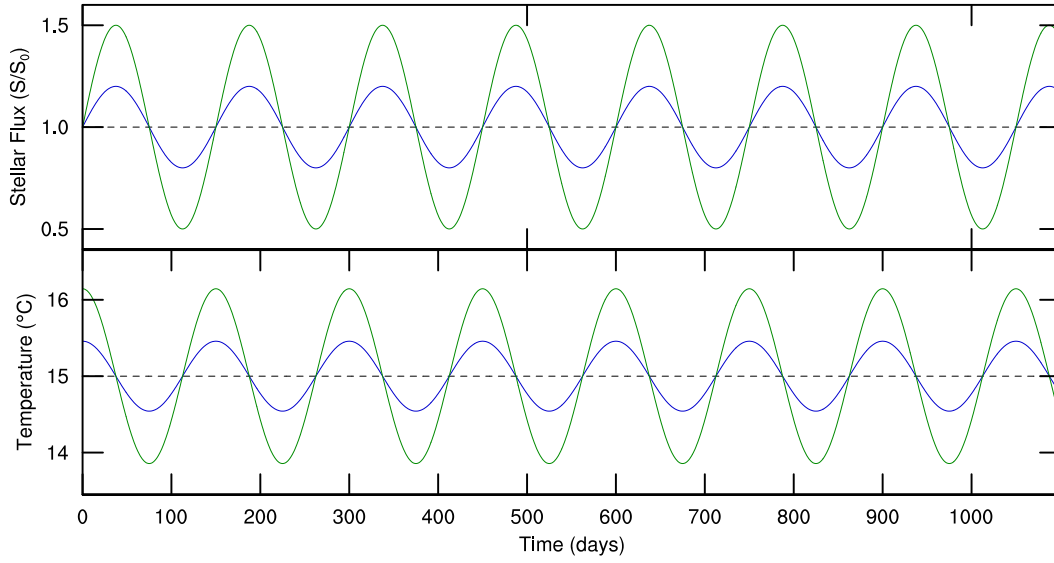


Figure 2. Steady state variations with time using the analytic EBM of the relative stellar flux (top) and mean planet temperature (bottom) for a fictitious $1 M_{\odot}$ primary and $0.5 M_{\odot}$ secondary case with $P_{bin} = 150$ days. Colored curves show a single star control case with $\kappa = 0$ (dashed black) and circumbinary cases with $\kappa = 0.2$ (blue) and $\kappa = 0.5$ (green).

variation and temperature response, which can substantially alter the magnitude of variation in T . In addition, the two parameters that influence temperature in this model are the amplitude of circumbinary forcing, κ , and the effective heat capacity, C . Physically, a larger value of κ corresponds to a larger flux variation from the binary pair. A larger value of C corresponds to a planet with greater average heat capacity that is less sensitive to time-varying changes in energy (such as a planet with a large fraction of ocean coverage).

The maximum temperature variation that can reasonably be attained through this model is given by the amplitude of the cosine term in Eq. (4). This maximum amplitude is shown in Fig. 3 as a “heat map” plot over the parameter space of C and κ , with $P_{bin} = 150$ days. The largest changes in temperature occur for planets with low effective heat capacity and a large amplitude of periodic forcing. Most of the parameter space shows only a few degrees total warming (and, analogously, the same amount of cooling), which corroborate previous studies [May and Rauscher, 2016; Popp and Eggl, 2017]. This suggests that the gyration effect is unlikely to substantially undermine the habitability of an Earth-like planet under the most typical conditions. But the upper-left quadrant of Fig. 3 also indicates that tens of degrees of variation could be possible for atmospheres with low effective heat capacity that experience large variations in stellar forcing. Under extreme conditions, circumbinary planets are capable of experiencing dramatic shifts in temperature.

This simple analytic model shows that a planet’s susceptibility to the circumbinary gyration effect is primarily controlled by its effective heat capacity. In the case of terrestrial planets, effective heat capacity is lowest for a dry land planet and increases for planets with greater ocean coverage and depth. The coefficients of the outgoing infrared radiative flux, A and B , can be altered to describe atmospheres of various compositions, based upon the net greenhouse warming, but these parameters do not affect the steady-state gyration effect described by Eq. (4). The gyration effect may therefore affect planetary habitability under certain scenarios. Circumbinary planets similar to Earth in terms of effective heat capacity (i.e., a similar ocean to land distribution), with low to moderate variation in instellation, may not experience significant variations in surface temperature. The gyration effect

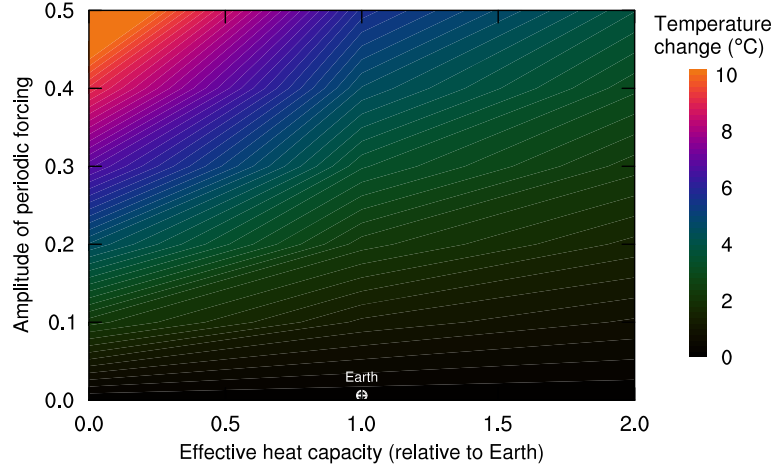


Figure 3. Maximum temperature change using the analytic EBM after reaching a steady state, shown over a parameter space of effective heat capacity and the amplitude of periodic forcing. The white circle indicates the heat capacity and constant forcing of present-day Earth.

cannot preclude habitability on such planets. Conversely, terrestrial planets with lower effective heat capacity (i.e., a lower ocean to land ratio) under larger instellation variation may find their global climates dominated by the changing flux from the binary. These extreme circumbinary systems may find themselves driven into climate regimes that diminish habitable conditions.

4 Numerical energy balance model

The analytic EBM used in the previous section demonstrates the significance of effective heat capacity as the primary planetary property that determines the response to circumbinary forcing. The analytic model assumes a fixed value of albedo, which thereby negates any ice-albedo feedback that could occur on such a planet; however planets that experience a circumbinary gyration effect with magnitude of a few degrees or greater could experience periodic changes in ice coverage that alter albedo and thus affect the total energy balance. The analytic model also constrains the planet to a single point, which neglects the contribution of meridional energy transport from equator to poles. We therefore continue our examination of the circumbinary gyration effect using a numerical EBM that accounts for ice-albedo feedback, meridional energy transport, and the effect of topography on effective heat capacity.

The numerical EBM [Haqq-Misra, 2014] is modified to include the circumbinary forcing term from Eq. (2). The energy balance equation for this model can then be written in terms of latitude, θ , as:

$$C \frac{\partial T}{\partial t} = S_0 (1 - \alpha) [1 + \kappa \sin(\omega t)] - (A + BT) + \frac{1}{\cos \theta} \frac{\partial}{\partial \theta} \left(D \cos \theta \frac{\partial T}{\partial \theta} \right). \quad (6)$$

The last term in Eq. (6) accounts for the efficiency of meridional energy transport by using D as a diffusive parameter, with $D = 0.38 \text{ W m}^{-2} \text{ K}^{-1}$ in this study as a fixed value applicable to present-day Earth conditions. Albedo is defined as a function of temperature so that $\alpha = 0.3$ for unfrozen land or ocean ($T \geq 263.15 \text{ K}$) and $\alpha = 0.663$ for any frozen surface ($T \leq 263.15 \text{ K}$). (Note that this threshold is ten degrees below freezing to indicate the formation of permanent surface ice.) The thermal emitted flux parameters are set to $A = 203 \text{ W m}^{-2}$ and $B = 2 \text{ W m}^{-2} \text{ }^\circ\text{C}^{-1}$. The EBM decomposes the planet into 18 equally-spaced latitudinal zones, assumes a starting surface temperature profile, and then numerically solves Eq. (6) by using a time step of $\Delta t = 8.64 \times 10^3 \text{ s} = 1 \text{ day}$. This model assumes a circular orbit for purposes of comparing directly with the analytic solution, while noting that planets

in circumbinary systems will necessarily have non-zero eccentricity. We initially keep planetary obliquity fixed at zero degrees in order to eliminate any seasonal effects, although we later consider the effect of seasons (following *Gaidos and Williams* [2004]) on circumbinary planets with Earth-like axial tilt.

Effective heat capacity, C , is defined in the numerical EBM as a function of both latitude and temperature, which represents the contributions from unfrozen land, unfrozen ocean, and ice-covered surface. Letting f_o and f_i represent the respective fraction of ocean and ice at each latitudinal zone, we can write the zonally averaged heat capacity as

$$C = (1 - f_i) C_l + f_o [(1 - f_i) C_o + f_i C_i], \quad (7)$$

where $C_l = 5.25 \times 10^6 \text{ J m}^{-2} \text{ K}^{-1}$ is the heat capacity of continental land, $C_o = 40 C_l = 2.1 \times 10^8 \text{ J m}^{-2} \text{ K}^{-1}$ is the heat capacity over a wind-mixed 50 m ocean layer, and $C_i = 2 C_l = 1.05 \times 10^7 \text{ J m}^{-2} \text{ K}^{-1}$ is the heat capacity over ice [Fairén et al., 2012]. Eq. (7) enables the numerical EBM to vary effective heat capacity according to surface conditions on the planet as a function of latitude.

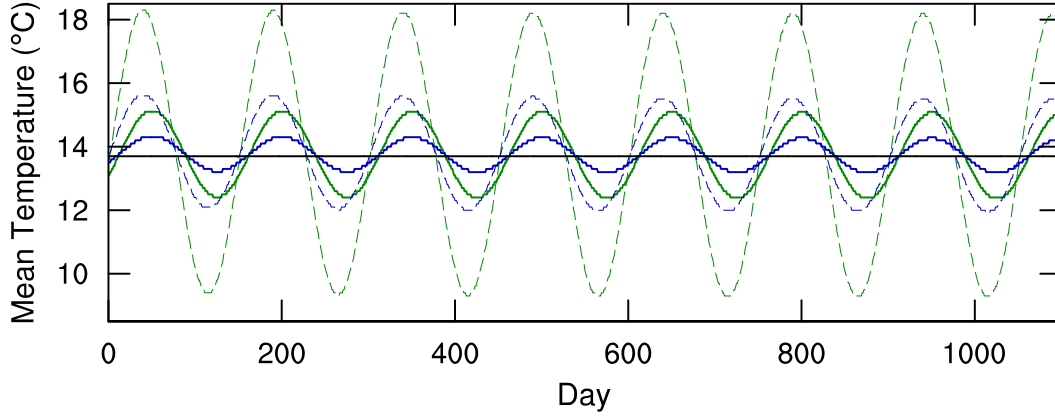


Figure 4. Steady state variations of mean planet temperature with time using the numerical EBM for a fictitious $1 M_{\odot}$ primary and $0.5 M_{\odot}$ secondary case with $P_{bin} = 150$ days. Colored curves show a single star control case with $\kappa = 0$ (dashed black) and circumbinary cases with $\kappa = 0.2$ (blue) and $\kappa = 0.5$ (green), all with zero obliquity. Solid curves indicate global aquaplanet conditions with no topography, while dashed curves indicate an equatorial supercontinent as topography.

4.1 Periodic temperature variations

Steady-state solutions of Eq. (6) are shown as mean temperature in Fig. 4 for the same $P_{bin} = 150$ day circumbinary system considered with the analytical model. The single star control case is shown as a black line on Fig. 4, along with circumbinary cases with moderate forcing ($\kappa = 0.2$, blue curves) and strong forcing ($\kappa = 0.5$, green curves). Solid curves correspond to global aquaplanet conditions with no land ($f_o = 1.0$), while dashed curves include topography as an equatorial supercontinent with ocean at the poles ($f_o = 0.7$). The aquaplanet cases plotted in Fig. 4 are comparable with the analytic solutions shown in Fig. 2, which show a temperature oscillation of about a degree for $\kappa = 0.2$ and about three degrees for $\kappa = 0.5$. The amplitudes of these aquaplanet solutions with the numerical EBM are slightly greater than the analytic EBM as the result of enhanced climate sensitivity from the inclusion of ice-albedo feedback and meridional energy transport. The equatorial supercontinent case shows a much larger amplitude of variation of about four degrees for $\kappa = 0.2$ and nearly ten degrees for $\kappa = 0.5$, due to the reduction in effective heat capacity along the planet's equatorial belt.

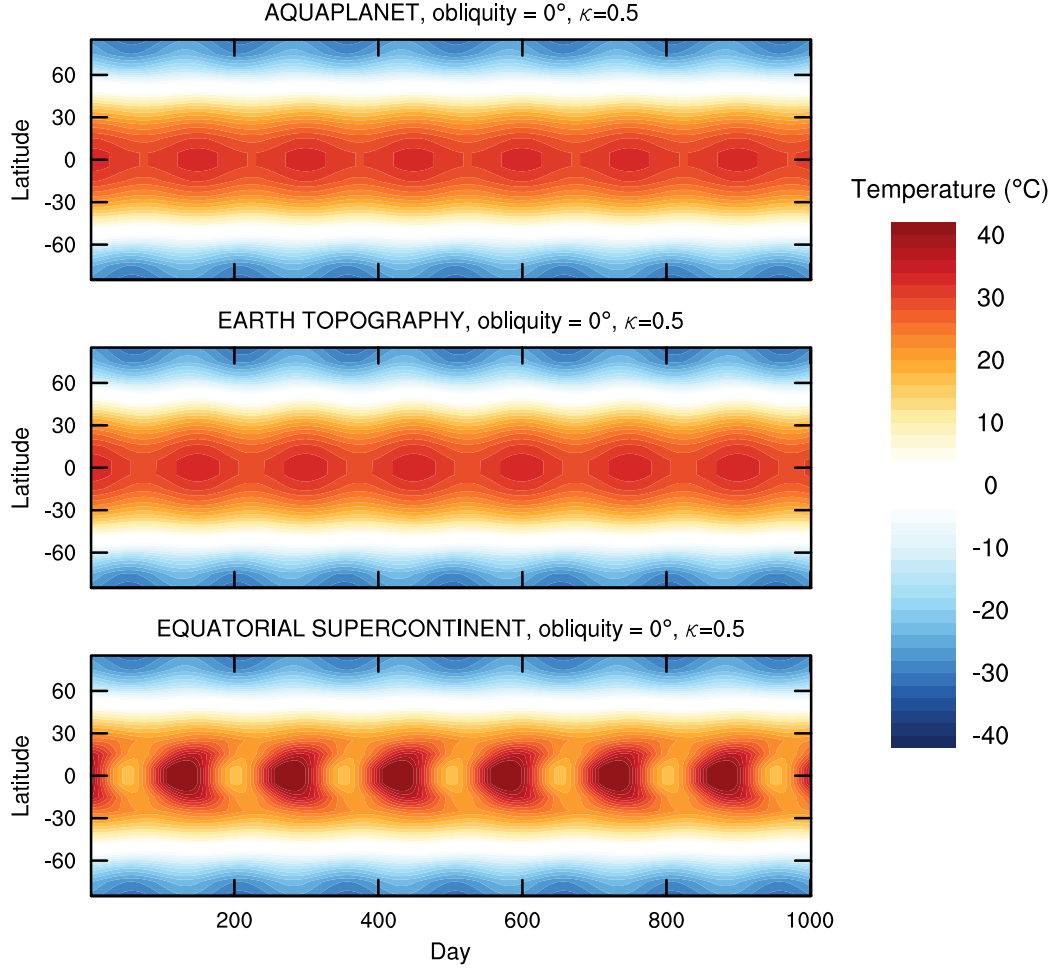


Figure 5. Steady state variations of the latitudinal distribution of planet temperature with time using the numerical EBM for a fictitious $1 M_{\odot}$ primary and $0.5 M_{\odot}$ secondary case with $P_{bin} = 150$ days. All calculations assume strong circumbinary forcing ($\kappa = 0.5$) and zero obliquity. Periodicity in temperature is evident for global aquaplanet conditions with no topography (top), Earth-like topography (middle), and an equatorial supercontinent as topography (bottom).

The choice of topography affects the amplitude and timing of temperature changes, as shown in Fig. 5 for the circumbinary case with strong forcing ($\kappa = 0.5$) and zero obliquity. The top row shows the latitudinal distribution of temperature with time for an aquaplanet, comparable to the solid green line on Fig. 4. The bottom row likewise shows latitudinal temperature with time for a planet with equatorial supercontinent topography, comparable to the dashed green line on Fig. 4. The middle row includes Earth topography, which assumes $f_o = 0.7$ but distributes the land across the northern and southern hemispheres. All cases show warm conditions along the equator and frozen conditions at latitudes greater than about 50 degrees. The aquaplanet and Earth topography cases both include a substantial fraction of ocean along the equator, which gives a higher heat capacity that allows equatorial latitudes to remain above freezing over a complete circumbinary period. The equatorial supercontinent case has complete land cover and thus a much lower heat capacity along the equator, which also remains above freezing at lower latitudes but shows a much greater amplitude of oscillation in temperature along the equator.

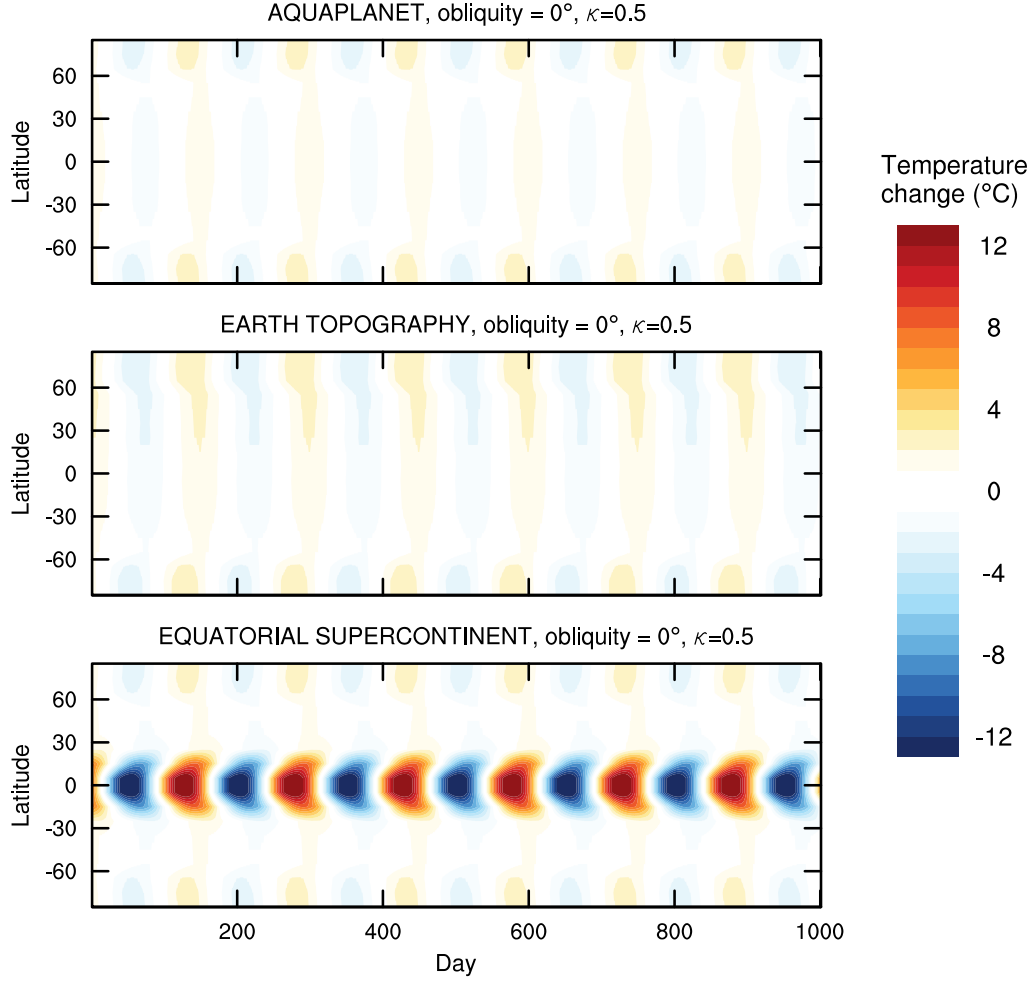


Figure 6. Steady state variations of the latitudinal distribution of planet temperature change with time using the numerical EBM for a fictitious $1 M_{\odot}$ primary and $0.5 M_{\odot}$ secondary case with $P_{bin} = 150$ days. All calculations assume strong circumbinary forcing ($\kappa = 0.5$) and zero obliquity. Periodic changes in temperature are evident for global aquaplanet conditions with no topography (top), Earth-like topography (middle), and an equatorial supercontinent as topography (bottom). The temperature difference is calculated by taking the three cases from Fig. 5 and subtracting the single-star temperature solutions from the EBM with the same respective topography.

The transient warming and cooling induced by the circumbinary effect is illustrated in Fig. 6. This figure shows the temperature change obtained by taking the three cases from Fig. 4 and subtracting the corresponding single-star temperature solutions of the numerical EBM. The difference shown in Fig. 6 indicates symmetric temperature variation of a few degrees for the aquaplanet (top row), with the greatest variation occurring at polar latitude where ice caps form, and asymmetric temperature variation for Earth topography (middle row) that reflects the larger concentration of land area in the northern hemisphere. The equatorial supercontinent topography (bottom row) shows changes of more than ten degrees along the equator, with relatively little variation in the northern and southern oceans. This is because the efficiency of the diffusive energy transport is enhanced over land compared to ocean (from Eqs. (6) and (7)), which results in an increase in the amplitude of temperature variation on areas with large land fractions and a decrease in variation over large

oceans. The lack of a seasonal cycle also causes higher latitudes to experience a lower amplitude of stellar forcing, which contributes to a smaller variation in temperature.

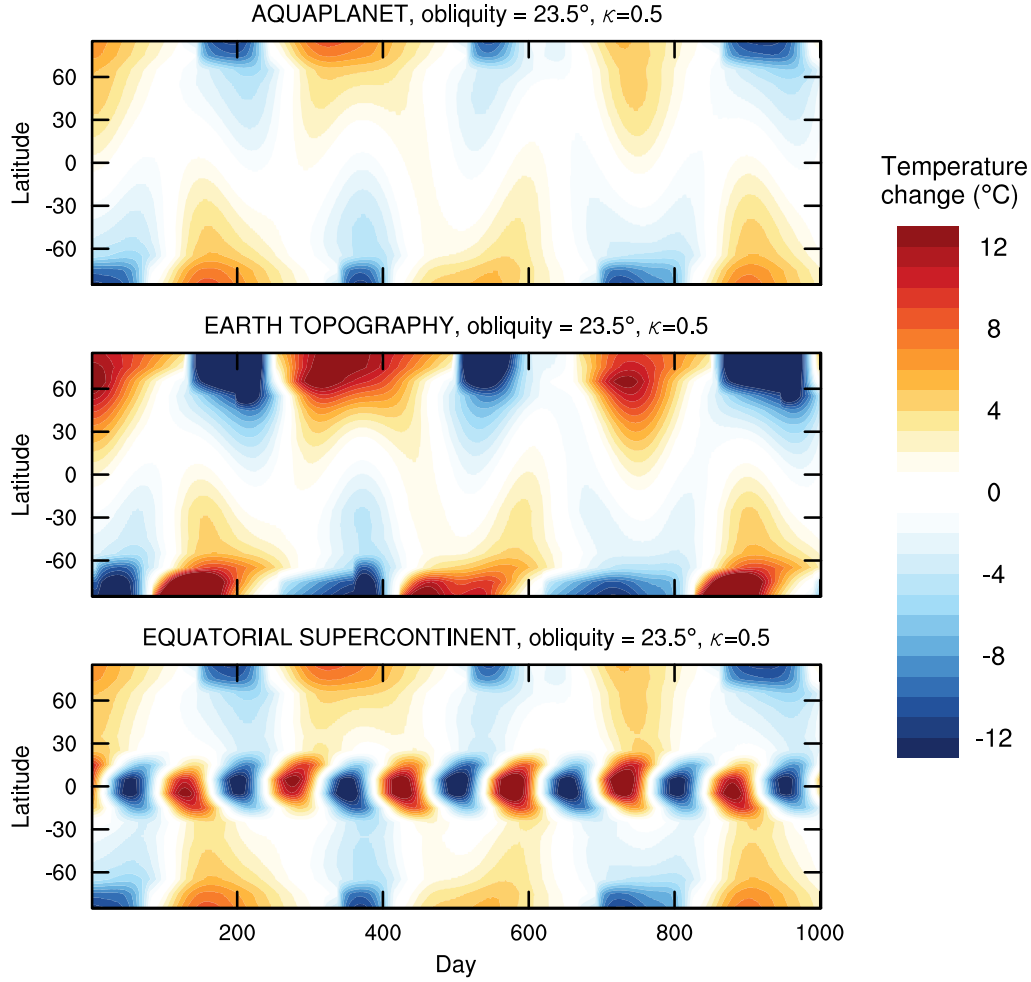


Figure 7. Steady state variations of the latitudinal distribution of planet temperature change with time using the numerical EBM for a fictitious $1 M_{\odot}$ primary and $0.5 M_{\odot}$ secondary case with $P_{bin} = 150$ days. All calculations assume strong circumbinary forcing ($\kappa = 0.5$) and 23.5° obliquity. Periodic changes in temperature are evident for global aquaplanet conditions with no topography (top), Earth-like topography (middle), and an equatorial supercontinent as topography (bottom). The temperature difference is calculated by subtracting the single-star temperature solutions from the circumbinary solutions from the EBM with the same respective topography.

This analysis has so far been restricted to a planet with zero obliquity, which keeps the maximum extent of incident stellar radiation focused along the equator. By contrast, a non-zero obliquity will result in a cycle that shifts the maximum in circumbinary variation from the equator toward the poles with the seasons [May and Rauscher, 2016]. We therefore consider a set of calculations similar to those shown in Fig. 6 but with Earth-like obliquity. The temperature change obtained for a circumbinary planet with 23.5° obliquity is shown in Fig. 7 for aquaplanet, Earth-like, and equatorial supercontinent topographies and strong circumbinary forcing ($\kappa = 0.5$). The aquaplanet case in Fig. 7 (top row) shows greater temperature change near the poles compared to the corresponding case in Fig. 6, due to the seasonal extremes experienced at the planet’s poles. Likewise, the Earth topography case (middle row) shows amplified temperature change near the poles compared to the

zero obliquity case, both of which are more extreme than the aquaplanet case due to the presence of continents in both hemispheres. The equatorial supercontinent case in Fig. 7 (bottom row) shows the most similarity with the corresponding case in Fig. 6, although the 23.5° obliquity case still shows seasonal variation of temperature near the poles. These results emphasize the strong control exerted by the ocean-to-land fraction on the temperature variation that results on an Earth-like planet from the circumbinary gyration effect.

The analytic EBM indicates that the amplitude of temperature variation from the circumbinary gyration effect is sensitive to the effective heat capacity (Fig. 3), but the numerical EBM illustrates that the latitudinal profile of heat capacity also exerts a strong control on the maximum amplitude of warming (Figs. 6 and 7). This occurs not only because of the reduced heat capacity of land compared to ocean but also because diffusive meridional energy transport is enhanced over land. This feature may also be relevant for planetary habitability, as large land areas (and thus any land-based life) on circumbinary planets are more likely to experience temperature variations from the gyration effect than large oceans.

4.2 Climate bistability

The bistability of Earth-like climates is a well-known feature of EBMs [North et al., 1981; Caldeira and Kasting, 1992] that also appears in many GCMs [DeConto and Pollard, 2003; Ishiwatari et al., 2007; Voigt and Marotzke, 2010; Wolf et al., 2017], with both warm and ice-covered solutions available at a given value of stellar flux. The left panels of Fig. 8 illustrate this classic hysteresis loop for 0° obliquity (top) and 23.5° obliquity (bottom), with the blue curve representing equilibrium EBM solutions initialized from ice-covered conditions and the red curve indicating solutions initialized from ice-free conditions. The dashed lines show transitions from an ice-covered to ice-free state (dashed red) and from an ice-free to ice-covered state (dashed blue). In general Fig. 8 describes a planet's climate state in terms of the relative warming and the previous climate state. This hysteresis loop indicates that large ice caps on Earth can remain stable until approximately 30 degrees, after which the planet falls into global glaciation. This transition is not immediately reversible but instead requires a significant increase in relative warming (either a change in stellar flux or, equivalently in this case, greenhouse gas forcing) before deglaciation can occur. On Earth, deglaciation from a global snowball condition seems to have occurred at least once, during the Neoproterozoic Era [Hoffman et al., 1998].

The 0° obliquity case in Fig. 8 also shows additional ice-free climate states in pink; this is known as the “small ice cap” solution, which describes the threshold at which a warming climate causes a small polar ice cap to become unstable and vanish. This small ice cap instability has been observed in other EBMs [North, 1984; Huang and Bowman, 1992] as well as some GCMs [Lee and North, 1995; Winton, 2006]; however, the small ice cap is not as ubiquitous in climate models as the more prominent large ice cap instability. For the 0° obliquity case, the small ice cap instability occurs at approximately 80 degrees, after which the planet transitions to an ice-free state. This transition is also not immediately reversible; if relative warming were to decrease on such a planet, then the climate would gradually cool and eventually fall into a large ice cap state.

Circumbinary planets show reduced bistability compared to their single star counterparts, as shown in the middle and right columns of Fig. 8. The cases with moderate forcing ($\kappa = 0.2$) show a reduction in the width of the hysteresis loop, which indicates a lower threshold for a frozen planet to deglaciate. This narrowing is even more pronounced in the strong forcing cases ($\kappa = 0.5$), which features an abrupt transition from a glacial state to a warm, but nearly ice-free, state. The temperature variation from the circumbinary gyration effect causes this narrowing of the hysteresis loop by reducing both the glaciation and deglaciation thresholds as the climate periodically exceeds mean temperature at all latitudes. The 0° obliquity cases show a wider hysteresis loop than the 23.5° obliquity cases, as the latter includes seasonal forcing that causes additional melting at the summer pole [Gaidos and Williams, 2004; May and Rauscher, 2016]. The increase in obliquity also causes the small ice cap instability to vanish in this model, even though the moderate forcing ($\kappa = 0.2$) circumbinary case retains a small ice cap solution at zero obliquity.

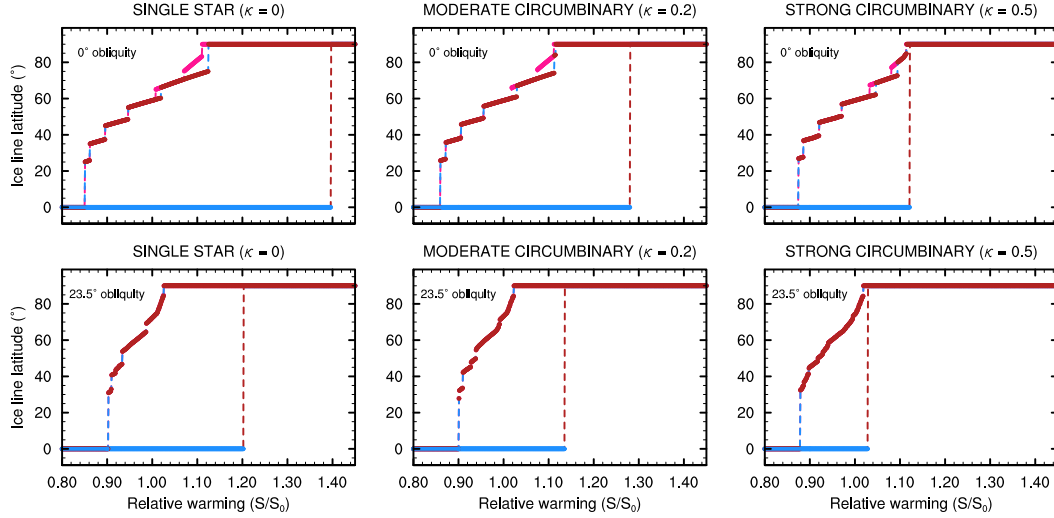


Figure 8. Hysteresis plots using the numerical EBM showing climate bistability for a planet with Earth-like topography orbiting a single star ($\kappa = 0$, left), a binary pair with moderate forcing ($\kappa = 0.2$, middle), and a binary pair with strong forcing ($\kappa = 0.5$, right). The top row shows cases with 0° obliquity and the bottom row shows cases with 23.5° obliquity. Climate states indicate solutions of the EBM when initialized with ice-covered (blue), ice-cap (red), and ice-free (pink) conditions. Dashed lines show discontinuous transitions between climate states. The width of the hysteresis loop between ice-covered and ice-free states narrows as the circumbinary gyration effect increases or as obliquity increases.

The zero obliquity cases may be less realistic for actual circumbinary planets, as the the orbital properties of the host stars and as the presence of other planets in the system can place constraints on a planet's obliquity. In particular, spin-orbit coupling in such a system can cause a circumbinary planet to enter a Cassini State that causes large variations in obliquity [Kostov et al., 2014; Forgan et al., 2015]. Increasing the obliquity beyond the present-day Earth value considered in this study would further increase the magnitude periodic temperature variation (Fig. 7) and reduce the width of the hysteresis loop (Fig. 8). Earth-like circumbinary planets within the liquid water habitable zone may therefore be less likely to be globally glaciated and more likely to exist in an ice-free or ice-cap state.

5 Discussion and Conclusions

We find that the habitability of circumbinary planets depends upon the ocean-to-land fraction of the surface, as well as the amplitude of forcing from the gyration effect. Terrestrial planets with larger land fractions than Earth, or a greater surface area of land at equatorial latitudes, should experience much greater shifts in temperature than planets with large ocean fractions. The lower effective heat capacity of land as well as the enhanced efficiency of meridional energy transport make such areas susceptible to greater changes in temperature from variations in instellation. This behavior occurs because the atmospheres of planets we have considered are largely transparent to incident instellation (which is mostly at short wavelengths), with atmospheric greenhouse gases absorbing primarily at longer infrared wavelengths. Such an assumption is generally valid for a wide range of plausible terrestrial planets, even with atmospheres several times more dense than present-day Earth. Circumbinary planets are expected to show reduced bistability, due to both the gyration effect as well as high obliquity (Fig. 8), which may suggest that such planets may more easily deglaciate from a frozen snowball state.

Our model calculations support the results of *Popp and Eggl* [2017], showing small temperature variations from the gyration effect, when we examine a planet with global ocean coverage (Figs. 6 and 7, top row). But when we include Earth-like land coverage or an equatorial supercontinent (Figs. 6 and 7, middle and bottom rows, respectively), we find that the lower effective heat capacity increases the extent of surface temperature variation. Such planets that experience a low to moderate variation in the circumbinary flux are likely to experience changes on a timescale analogous to a seasonal cycle, which may not necessarily preclude habitability. Any Earth-like circumbinary planets that are eventually discovered may therefore be attractive candidates for spectroscopic characterization in the quest to discover potential biosignatures with the next generation of space telescopes [*Kiang et al.*, 2018].

Circumbinary planets that lack large oceans are prone to experience a greater amplitude of temperature variation. The equatorial supercontinent cases shown in Figs. 5, 6 and 7 exhibit periodic variation on a scale analogous to seasonal cycles but do not freeze along the equator, so habitability cannot be precluded on such planets. However, the equatorial supercontinent case is not a pure land planet and includes ocean at the poles, with $f_o = 0.7$. The numerical EBM became numerically unstable at lower values of lower values of f_o , which indicates the high sensitivity of this model to the planet's effective heat capacity. Planets with much larger land fractions could experience even greater variation in temperature that could lead to freezing conditions along the equator. While such changes could pose challenges for biology, the freeze-thaw cycle on such planets could instead provide a selection pressure that helps to drive biological evolution. The magnitude of temperature change on such planets will help predict whether such behavior is a detriment to habitability and will require more detailed calculations using a GCM tailored to the particular system.

M-dwarf stars emit a substantial fraction of radiation at infrared wavelengths, so a planet orbiting a circumbinary pair of M-dwarf stars would be able to absorb a greater fraction of incident instellation with its atmosphere. A planet with a sufficiently dense atmosphere around such a pair of low-mass stars might even absorb enough incoming radiation that periodic variations on the surface are damped and overall less sensitive to the ocean fraction. This would also drive complex behavior, such as changes in the substellar cloud deck, that cause further feedbacks on climate. Testing this scenario will require calculations with a GCM that include stellar spectra from a low-mass circumbinary pair.

This study has explored the extent of periodic temperature variation on Earth-like circumbinary planets; however, diurnal variations in climate cannot be captured with either the analytic or numerical EBM. Similarly, the representation of topography in the numerical EBM is based only on the ocean-to-land fraction at each latitude band, with no regard to the distribution of land with longitude. Previous GCM studies of circumbinary planets have assumed uniform surface conditions, and focus on spatially averaged quantities, but localized warming effects over the diurnal cycle and across continents could limit habitability in certain regions on the surface; for example, the surface habitability limits suggested by *Sherwood and Huber* [2010] are based upon the ability for humans and other mammals to efficiently dissipate metabolic heat. Further work with GCMs will therefore provide quantitative constraints on the expected climates of terrestrial circumbinary planets that experience extreme forcing from their binary star host.

Appendix: Analytic Energy Balance Model

This appendix provides the analytic solution of the energy balance model equation with sinusoidal forcing in Eq. (3). We begin by writing the homogeneous part of Eq. (3),

$$\frac{dT}{dt} + \frac{B}{C}T = 0. \quad (8)$$

The solution to Eq. (8) gives $T_g(t) = X \exp(-Bt/C)$, where X is a constant. This is the general solution to Eq. (3). We next find the particular solution of Eq. (3) by assuming a solution in the form $T_p(t) = Y \sin(\omega t) + Z \cos(\omega t) + W$, where Y , Z , and W are constants. Substituting this expression

for $T_p(t)$ into Eq. (3) gives

$$[BY - \omega CZ] \sin(\omega t) + [BZ + \omega CY] \cos(\omega t) = S_0(1 - \alpha)[1 + \kappa \sin(\omega t)] - A - BW. \quad (9)$$

Setting the constant terms of Eq. (9) equal to each other gives the value of W , as

$$W = \frac{S_0(1 - \alpha) - A}{B}. \quad (10)$$

The constants Y and Z can be found by equating the coefficients of the trigonometric functions on both sides of Eq. (9), which gives the values

$$Y = \frac{S_0(1 - \alpha)\kappa B}{\omega^2 C^2 + B^2}, \quad (11)$$

and

$$Z = \frac{-S_0(1 - \alpha)\kappa \omega C}{\omega^2 C^2 + B^2}. \quad (12)$$

The full solution to Eq. (3) is given as the sum of the general and particular solutions, $T(t) = T_g(t) + T_p(t)$. We can now write this solution as

$$T(t) = X \exp\left(\frac{-Bt}{C}\right) + Y \sin(\omega t) + Z \cos(\omega t) + W. \quad (13)$$

The values of Y , Z , and W are known. To find the value of X , we assume $T(t) = T_0$ at $t = 0$. This boundary condition reduces Eq. (13) to $T_0 = X + Z + W$, which gives

$$X = T_0 + S_0(1 - \alpha) \left[\frac{\kappa \omega C}{\omega^2 C^2 + B^2} - \frac{1}{B} \right] + \frac{A}{B}. \quad (14)$$

This solution can be verified by substituting Eq. (13) into Eq. (3) using the respective values of W , X , Y , and Z from Eqs. (10), (14), (11), and (12).

We can simplify Eq. (13) by examining the steady state solution as t becomes large and the general solution to Eq. (3) vanishes, $T_g(t) \approx 0$. The particular solution to Eq. (3), $T_p(t)$, can be reduced by noting that $\omega C \gg B$ for the range of parameters considered in this study. By first rewriting the particular solution as $T_p = \sqrt{Y^2 + Z^2} \cos(\omega t - \arctan \frac{Z}{Y}) + W$, we arrive at an expression for the steady state solution to Eq. (3):

$$T(t) \approx \frac{S_0(1 - \alpha)\kappa}{\omega C} \cos(\omega t) + T_0. \quad (15)$$

Acknowledgments

The data used for this paper can be accessed at <https://doi.org/10.6084/m9.figshare.10279790>. The authors gratefully acknowledge funding from the NASA Habitable Worlds program under award 80NSSC17K0741. J.H., E.T.W., and R.K.K. also acknowledge funding from the Virtual Planetary Laboratory under NASA award 80NSSC18K0829, and R.K.K. and V.K. acknowledge funding from the Sellers Exoplanet Environments Collaboration. W.F.W. gratefully thanks John Hood Jr. for his support of exoplanet research at SDSU. Any opinions, findings, and conclusions or recommendations expressed in this material are those of the authors and do not necessarily reflect the views of NASA.

References

- Abe, Y., A. Abe-Ouchi, N. H. Sleep, and K. J. Zahnle (2011), Habitable zone limits for dry planets, *Astrobiology*, 11(5), 443–460.
- Bolmont, E., A.-S. Libert, J. Leconte, and F. Selsis (2016), Habitability of planets on eccentric orbits: Limits of the mean flux approximation, *Astronomy & Astrophysics*, 591, A106.
- Caldeira, K., and J. F. Kasting (1992), Susceptibility of the early earth to irreversible glaciation caused by carbon dioxide clouds, *Nature*, 359(6392), 226.

- Cuntz, M. (2013), S-type and p-type habitability in stellar binary systems: A comprehensive approach. i. method and applications, *The Astrophysical Journal*, 780(1), 14.
- Cuntz, M. (2015), S-type and p-type habitability in stellar binary systems: a comprehensive approach. ii. elliptical orbits, *The Astrophysical Journal*, 798(2), 101.
- DeConto, R. M., and D. Pollard (2003), Rapid cenozoic glaciation of antarctica induced by declining atmospheric co₂, *Nature*, 421(6920), 245.
- Doyle, L. R., J. A. Carter, D. C. Fabrycky, R. W. Slawson, et al. (2011), Kepler-16: A Transiting Circumbinary Planet, *Science*, 333, 1602.
- Dressing, C. D., D. S. Spiegel, C. A. Scharf, K. Menou, and S. N. Raymond (2010), Habitable climates: the influence of eccentricity, *The Astrophysical Journal*, 721(2), 1295.
- Dvorak, R. (1984), Numerical experiments on planetary orbits in double stars, in *The Stability of Planetary Systems*, pp. 369–378, Springer.
- Fairén, A., J. Haqq-Misra, and C. McKay (2012), Reduced albedo on early mars does not solve the climate paradox under a faint young sun, *Astronomy & Astrophysics*, 540, A13.
- Forgan, D. (2013), Assessing circumbinary habitable zones using latitudinal energy balance modelling, *Monthly Notices of the Royal Astronomical Society*, 437(2), 1352–1361.
- Forgan, D. H., A. Mead, C. S. Cockell, and J. A. Raven (2015), Surface flux patterns on planets in circumbinary systems and potential for photosynthesis, *International Journal of Astrobiology*, 14(3), 465–478.
- Gaidos, E., and D. Williams (2004), Seasonality on terrestrial extrasolar planets: inferring obliquity and surface conditions from infrared light curves, *New Astronomy*, 10(1), 67–77.
- Georgakarakos, N., and S. Eggl (2019), On the enlargement of habitable zones around binary stars in hostile environments, *Monthly Notices of the Royal Astronomical Society: Letters*, 487(1), L58–L60.
- Haghighipour, N., and L. Kaltenegger (2013), Calculating the habitable zone of binary star systems. ii. p-type binaries, *The Astrophysical Journal*, 777(2), 166.
- Haqq-Misra, J. (2014), Damping of glacial-interglacial cycles from anthropogenic forcing, *Journal of Advances in Modeling Earth Systems*, 6(3), 950–955.
- Hoffman, P. F., A. J. Kaufman, G. P. Halverson, and D. P. Schrag (1998), A neoproterozoic snowball earth, *science*, 281(5381), 1342–1346.
- Holman, M. J., and P. A. Wiegert (1999), Long-term stability of planets in binary systems, *The Astronomical Journal*, 117(1), 621.
- Huang, J., and K. P. Bowman (1992), The small ice cap instability in seasonal energy balance models, *Climate dynamics*, 7(4), 205–215.
- Ishiwatari, M., K. Nakajima, S.-i. Takehiro, and Y.-Y. Hayashi (2007), Dependence of climate states of gray atmosphere on solar constant: From the runaway greenhouse to the snowball states, *Journal of Geophysical Research: Atmospheres*, 112(D13).
- Kane, S. R., and N. R. Hinkel (2012), On the habitable zones of circumbinary planetary systems, *The Astrophysical Journal*, 762(1), 7.
- Kasting, J. F., D. P. Whitmire, and R. T. Reynolds (1993), Habitable zones around main sequence stars, *Icarus*, 101(1), 108–128.
- Kiang, N. Y., S. Domagal-Goldman, M. N. Parenteau, D. C. Catling, Y. Fujii, V. S. Meadows, E. W. Schwieterman, and S. I. Walker (2018), Exoplanet biosignatures: At the dawn of a new era of planetary observations, *Astrobiology*.
- Kopparapu, R. K., R. Ramirez, J. F. Kasting, V. Eymet, T. D. Robinson, S. Mahadevan, R. C. Terrien, S. Domagal-Goldman, V. Meadows, and R. Deshpande (2013), Habitable zones around main-sequence stars: new estimates, *The Astrophysical Journal*, 765(2), 131.
- Kopparapu, R. K., R. M. Ramirez, J. SchottelKotte, J. F. Kasting, S. Domagal-Goldman, and V. Eymet (2014), Habitable Zones around Main-sequence Stars: Dependence on Planetary Mass, *ApJL*, 787, L29, doi:10.1088/2041-8205/787/2/L29.
- Kostov, V. B., P. R. McCullough, J. A. Carter, M. Deleuil, R. F. Díaz, D. C. Fabrycky, G. Hebrard, T. C. Hinse, T. Mazeh, J. A. Orosz, et al. (2014), Kepler-413b: a slightly misaligned, neptune-size transiting circumbinary planet, *The Astrophysical Journal*, 784(1), 14.

- Lee, W.-H., and G. North (1995), Small ice cap instability in the presence of fluctuations, *Climate dynamics*, 11(4), 242–246.
- Mason, P. A., J. I. Zuluaga, J. M. Clark, and P. A. Cuartas-Restrepo (2013), Rotational Synchronization May Enhance Habitability for Circumbinary Planets: Kepler Binary Case Studies, *ApJL*, 774, L26, doi:10.1088/2041-8205/774/2/L26.
- May, E., and E. Rauscher (2016), Examining tatooine: Atmospheric models of neptune-like circumbinary planets, *The Astrophysical Journal*, 826(2), 225.
- North, G. R. (1984), The small ice cap instability in diffusive climate models, *Journal of the atmospheric sciences*, 41(23), 3390–3395.
- North, G. R., R. F. Cahalan, and J. A. Coakley Jr (1981), Energy balance climate models, *Reviews of Geophysics*, 19(1), 91–121.
- Orosz, J. A., W. F. Welsh, N. Haghighipour, B. Quarles, D. R. Short, S. M. Mills, S. Satyal, G. Torres, E. Agol, D. C. Fabrycky, et al. (2019), Discovery of a third transiting planet in the kepler-47 circumbinary system, *The Astronomical Journal*, 157(5), 174.
- Pecaut, M. J., and E. E. Mamajek (2013), Intrinsic colors, temperatures, and bolometric corrections of pre-main-sequence stars, *The Astrophysical Journal Supplement Series*, 208(1), 9.
- Pecaut, M. J., E. E. Mamajek, and E. J. Bubar (2012), A revised age for upper scorpius and the star formation history among the f-type members of the scorpius-centaurus ob association, *The Astrophysical Journal*, 746(2), 154.
- Popp, M., and S. Eggl (2017), Climate variations on earth-like circumbinary planets, *Nature communications*, 8, 14,957.
- Sherwood, S. C., and M. Huber (2010), An adaptability limit to climate change due to heat stress, *Proceedings of the National Academy of Sciences*, 107(21), 9552–9555.
- Stephens, G. L., D. O'Brien, P. J. Webster, P. Pilewski, S. Kato, and J.-I. Li (2015), The albedo of earth, *Reviews of Geophysics*, 53(1), 141–163, doi:10.1002/2014RG000449.
- Voigt, A., and J. Marotzke (2010), The transition from the present-day climate to a modern snowball earth, *Climate dynamics*, 35(5), 887–905.
- Wang, Z., and M. Cuntz (2019a), S-type and p-type habitability in stellar binary systems: A comprehensive approach. iii. results for mars, earth, and super-earth planets, *The Astrophysical Journal*, 873(2), 113.
- Wang, Z., and M. Cuntz (2019b), S-type and p-type habitable zones of stellar binary systems: Effect of the planetary mass, *Research Notes of the AAS*, 3(5), 70.
- Way, M. J., and N. Georgakarakos (2017), Effects of variable eccentricity on the climate of an earth-like world, *The Astrophysical Journal Letters*, 835(1), L1.
- Welsh, W. F., and J. A. Orosz (2018), Two suns in the sky: The Kepler circumbinary planets, *Handbook of Exoplanets*, Edited by Hans J. Deeg and Juan Antonio Belmonte. Springer Living Reference Work, ISBN: 978-3-319-30648-3, 2017, id. 34.
- Welsh, W. F., J. A. Orosz, J. A. Carter, D. C. Fabrycky, et al. (2012), Transiting circumbinary planets Kepler-34 b and Kepler-35 b, *Nature*, 481, 475–479, doi:10.1038/nature10768.
- Winton, M. (2006), Does the arctic sea ice have a tipping point?, *Geophysical Research Letters*, 33(23).
- Wolf, E. T., A. L. Shields, R. K. Kopparapu, J. Haqq-Misra, and O. B. Toon (2017), Constraints on climate and habitability for earth-like exoplanets determined from a general circulation model, *The Astrophysical Journal*, 837(2), 107.